

Response to Referee #1

Anonymous Referee #1

Received and published: 24 September 2018

General Comments:

Overall, the manuscript investigates the resonant period of the Gulf of Thailand (GOT) via numerical experiments and tries to establish a conceptual understanding of resonance in the gulf over two-channel model. The authors found that the resonant period of the GOT is closely related to that of the South China Sea body (SCSB) and is close to the period of the major diurnal tide, K1. They speculate that the resonance of the SCSB has a critical impact on the resonance of the GOT. On contrary, the resonance of the GOT has little influence on the resonance of the SCSB. I suggest that though this work seems to present interesting results speculating the interconnection of resonance between coastal bays and deep sea. However, the substantial analysis/discussion for convincing their findings/conclusions are inadequate and not up to the standard of the journal. For consideration of OS editor, some critical issues are addressed below:

Reply: We sincerely thank the referee for his careful reading of our manuscript and comments. We have revised this paper and addressed all these comments; our responses are given below.

In this response, the referee's comments are copied in black, our replies are shown in red, and the following abbreviations are used:

R1 – Revision #1 - an updated manuscript, which will be submitted as a supplement to this response.

Specific Comments:

1. Theoretically, the characteristic of the effective region for the resonance of long waves in the semi-enclosed sea can be calculated via the phase speed. For the GOT, the effective length of the basin for resonance of the diurnal tides can be approximately 1700 km. Besides, the co-tidal chart for K1 tide in the gulf suggests more precision length such as 1500 km. From this information, the resonant periods for the fundamental and first mode would be calculated as 73.8 and 24.61 hours (based on semi-enclosed basin formula). From these numbers, we could say that the period of diurnal tides in the gulf can be predominated by influence of the first mode instead of the fundamental mode. The role of the quarter wavelength resonant theory on tidal resonance in the GOT is insignificant and is easy to prove. However, this issue tends to be highlighted in the abstract and conclusion of the manuscript. But, it does not represent a substantial contribution to scientific progress in oceanography.

Reply: The GOT is a subsidiary gulf of the SCS, and the SCS is mainly composed of deep-sea basin and continental shelf (Figure 1). The SCS deep basin (abbreviated as SCSDB, where the water depth is more than 500 m, the blue line in Figure 1) connects with the GOT through the Sunda shelf (abbreviated as SS, where the water depth is less than 500 m). The average depth of the SCSDB is 2500 m, and the average depth of the SS and GOT are 66 m and 36 m, respectively. The water depth from the SCSDB to the SS varies dramatically (Figure 1).

The average depth within 1700 km (the length of the red line in Figure 1) of the semi-enclosed sea area is 173 m, of which the average depths of the GOT and SS are respectively 36 m and 66 m, and the average depth of a small part of the SCSDB is approximately 1000 m. According to the semi-closed basin formula, the resonance period should be approximately 15 hours, not 24 hours. If the range of 1700 or 1500 km is considered covering the whole continental shelf (including GOT and SS), its average depth is only 46 m and its resonance period is between 26 and 29 hours, not 24 hours.

Furthermore, in Cui et al. (2015), we find that the resonant period of the SCSDB is approximately one

day because the one-quarter wavelength resonance in the SCSB. In this paper, we carried out two experiments by changing the depth of SCSB; the depths are one half and two times that of the real depth, and we find that the resonant frequencies (periods) are approximately 0.5 cycle/day (period is 43 hours) and 1.5 cycle/day (period is 16 hours), respectively. The experimental results are consistent with those from the one-quarter wavelength of the SCSB. Again, it is proved that the strong diurnal tide in the SCSB is caused by the quarter-wavelength resonance, so the SCSB (covering the SS and SCSDB) can be regarded as a system subject to the one-quarter wavelength resonance.

Both the GOT and the Gulf of Tonkin are subsidiary gulfs of the SCS, and the strong diurnal tide in the Gulf of Tonkin is caused by the quarter-wavelength resonance (Cui et al, 2015; Fang et al, 1999). We speculate whether the strong diurnal tide in the GOT can be explained by the quarter-wavelength resonance, but we find that it cannot. We don't know the reasons for the strong response around one cycle/day in the GOT. Since the tidal energy of the GOT comes mainly from the SCS, we speculate that the strong response in the GOT may be related to the SCS. In R1, we conclude that the GOT does have a large amplitude response around one cycle/day, and the results indicate that is just a passive response of the gulf to the increased amplitude of the SCSB along its southern boundary.

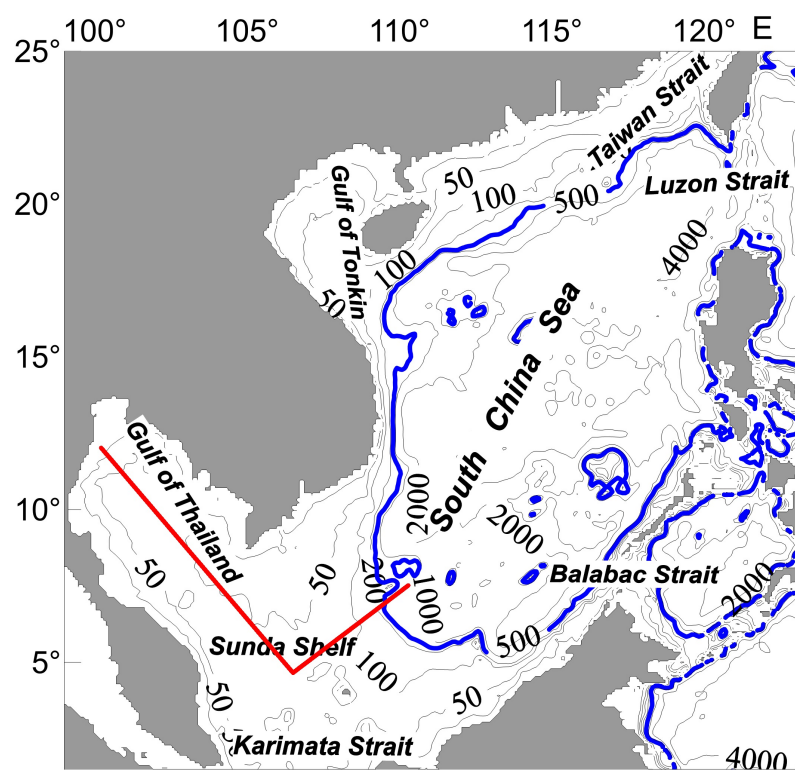


Figure 1. The length of the red line 1 is 1700 km; the blue line shows the 500 m isobath.

2. I wonder why the length of the GOT system is limited by the 660 km. The mentioned length may represent only the territorial sea of Thailand but does not involve the effective resonator system for tidal waves in true nature. Contrary, the size of the effective system should be larger as the entire western shelf of the South China Sea or Sunda Shelf (see the previous comment). Therefore, I suggest that the perception of a basin resonance oscillator and the dynamics of tidal waves in the GOT, the division of the computational domain, especially, the judgment of the authors for the application of classic quarter wavelength resonant theory for determining a diurnal resonant period of the GOT are altogether possible misconceptions.

Reply: Please kindly see the previous reply.

3. There are several resonance mechanisms (standing waves or basin mode and shelf mode) that might control oscillation of sea levels in the GOT system. Entirely, the impact of the standing waves modes associated with the period of approximately 24 hours is mostly accounted for. It is recognized that their modal structure distribution (nodal and anti-nodal bands) along the major axis of the system (the distance from the inner GOT to Kalimata strait, NS mode).

Reply: The SCSB plays a decisive role in the response peak in the GOT at the frequency of one cycle/day, and one-quarter wavelength of this frequency is approximately equal to the length of the SCSB, which leads a significant peak at the south of the SCSB, where is also the entrance to the GOT. The significant amplitude at the entrance of the GOT causes the GOT to have a strong response at the frequency of one cycle/day. The large amplitude in the GOT at this frequency is just a passive response to the increased amplitude caused by the one-quarter wavelength resonance in the SCSB.

Supported by the geometry defined by the distance from the Malaysia Peninsular to the eastern of the Taiwan Strait, the modal structure of mentioned period may also be fitted into the SCSB. But, it should have a different modal structure (East-West, EW mode). The existence of the mentioned modal structures revealed in the manuscript.

Reply: Please kindly see the previous reply.

Besides, the experiment in determining the effect of bottom topographies of the SCSB on the resonant response of the GOT is presented. As present in this part of the results, it seems that the consistency of the resonant periods are the main reason to judge that the GOT is not an independent sea area regarding tidal resonance. On the other hand, the amplification mechanism is not involved although the response (amplitude gain) of the GOT is probably higher than that of the SCSB (See Exp. 3 Result). The real phenomenon similar to the Exp.3 can be such as the resonance of M2 in the Bay of Bengal, Andaman seas and Malaca Strait.

Reply: Please kindly see the previous reply.

The part of the deeper and shallow sea of the mentioned system may have the same resonant period but amplification become more intensified near the shelf zone. Indeed, the resonance of the Andaman seas and Malaca Strait are not independent from the Bay of Bengal. But, they have the locality regarding the modal structure and amplification processes. Importantly, we might explain dynamic of tidal waves in the mentioned area as an influence of a combined-role of basin and local resonance modes. I suggest that this concept would also explain the interconnection of the GOT and SCSB. Hence, I reject that judgment as mentioned above because the locality of the GOT and the SCSB are found in their results.

Reply: Please kindly see the previous reply.

Moreover, for the idealized model part, the authors only show preliminary results that mostly identical to the numerical experiment. They do not present some discussion showing the benefit of the model to gain more comprehension of the tidal resonance in the GOT.

Reply: We added a new part containing content about this idealized model in R1 as follows: "If we apply the quarter-wavelength resonance theory to channel 1, we can obtain resonant frequencies of 0.99 d^{-1} . If we apply the quarter-wavelength and three-quarter-wavelength resonance theories to channel 2 we can obtain resonant frequencies of 0.61 and 1.84 d^{-1} , respectively. Therefore, we can conclude that the major peaks around the frequency of 1.04 d^{-1} in Figure 6 are caused by resonance in channel 1. This indicates that channel 1 plays a determinative role in the two-channel system. Similarly, we can also conclude that the secondary and third peaks around the frequencies of 0.55 and 1.85 d^{-1} in Figure 6 are caused by resonances in channel 2, associated with the quarter-wavelength and three-quarter-wavelength

resonances. Although the frequencies of the peaks shown in Figure 6 correspond well with those estimated based on the quarter-wavelength and three-quarter-wavelength theories, there are small discrepancies. This is due to the connection of the two channels. In fact, the resonant frequencies of the two-channel system also depend on the depth ratio of two channels, as shown in Eq. (14). In comparison to channel 2, the secondary, especially the third peak, in channel 1 is much more less significant. This can be explained as follows: The tidal incident wave from the channel 1 partially enters channel 2 across the steep topography at $x = 0$, and here, the rest of the wave is reflected. The reflected wave is superimposed with the incident wave, and tidal resonance occurs around the frequency of 1.04 d^{-1} . That is, the steep topography at $x = 0$ acts as a wall for channel 1, which causes the quarter-wavelength resonance to occur in the channel. Furthermore, the steep topography can also block most energy of the wave in channel 2 from entering channel 1. Therefore, the relatively large amplitudes in channel 2 at frequencies around 0.55 d^{-1} and 1.85 d^{-1} are not obvious in channel 1 under the action of friction”.

Response to Dr D.J. Webb (Referee)

Received and published: 29 October 2018

The oceans and marginal seas around South-east Asia are unusual in that the diurnal tides are often much more significant than in the rest of the world's ocean. In this paper the tides of the Gulf of Thailand are investigated to see how resonances enhance the tides of the region. The main result is that the high diurnal tides are not due to a resonance of the Gulf of Thailand but that they are probably due to a quarter wave resonance of the South China Sea. The paper builds on the model study of Cui et al (2015) but also includes an analytic 1-D model which supports the quarter-wave hypothesis. The paper is well written and easy to understand and although I have some serious criticisms of the work I would like to commend the authors on the standard of their discussion paper.

Reply: Dear Dr. Webb, we sincerely thank you for your careful reading of our manuscript and your constructive comments and suggestions, which are of great help in improving our study. We have addressed all these comments; our responses are given below.

In this response, your comments are copied in black, our replies are shown in red, and the following abbreviations are used:

R1 – Revision #1 - an updated manuscript, which will be submitted as a supplement to this response.

1. Abstract.

After reading the paper and that of Cui et al (2015) it seems obvious that it is the South China Sea which is responsible for the resonance. Thus changing the depth of the South China Sea changes the frequency of the resonance (fig 2) and the analytic resonance around 1 cy/day comes for the $\cos(\beta_1 L_1)$ term in the equation on line 159. However, the abstract says that the resonant period of the Gulf of Thailand is itself close to 1 cycle/day - which is incorrect.

It would be more correct to say that the South China Sea and the surrounding sea together have a resonance around 1 cycle/day which is primarily due to the South China Sea having very close to a quarter wavelength standing wave at this frequency. Although the Gulf of Thailand does have a large amplitude response around 1 cycle per day the results indicate that this is just a passive response of the Gulf to the increased amplitude of the main South China Sea wave along the Gulf's southern boundary.

Reply: We agree with this comment and have added the following sentence in the abstract: "We find that the resonant frequency around 1 cycle per day in the main area of the South China Sea can be explained with the quarter-wavelength theory, and the large-amplitude response at this frequency in the Gulf of Thailand is basically a passive response of the gulf to the increased amplitude of the wave in the southern portion of the main area of the South China Sea".

2. Lines 19, 22, 24

It would help if the geographical features Taiwan Strait, Mindoro Strait, Balabac Strait and any others referred to in the text were included in figure 1.

Reply: These geographical names have been added to Fig. 1 as suggested.

3. Line 32

In some parts of the literature there is a tendency to refer to resonances in terms of their period. However because the angular velocity of resonances (or their frequencies) often form an arithmetic series corresponding $1/4, 3/4, 5/4$, etc wavelengths I would recommend replacing periods here by angular velocities (or frequencies), possibly with the periods in brackets for those that need them.

Reply: This comment has been adopted. We have changed the units of period to those of frequency in R1.

4. Line 47-48

It is not that the resonant periods are related but that the two features are parts of the same resonance, the angular velocity of the resonance being determined primarily by the physical properties of the South China Sea.

Reply: We accept this point of view. Accordingly, these statements have been changed to “we investigate the reasons for the GOT to have a strong response around the frequency of one cycle per day and how the physical properties of the SCSB primarily determine the resonances of both the SCSB and the GOT”.

5. Line 72: The Numerical Model

It is only in the code availability section that you say that you use the Princeton Ocean Model. I think this needs to be mentioned earlier in the paper as there are many types of ocean model of varying quality. The Princeton Model is well known and is usually acknowledged to be of good quality. However, it includes many options and parameters so, as in any other realistic model study, it is important to show that the version in use can realistically represent the actual tides in the region being studied. For this reason the paper needs an example of the model K1 (and/or O1) tides of the region and comparison with actual tidal observations either in the form of a chart or in the form of comparisons at key tide gauge positions. I realise that Cui et al (2015) did not do this, but if I had refereed their paper I would have made the same point.

Reply: We added the content of the numerical simulation of the tide K₁, and the results are compared with the tidal gauges. See the R1, Subsection 2.2.

You could also do with figures showing the flux of tidal energy for both the realistic K1 tidal forcing and with a constant amplitude on the boundary as in your test experiments, to show that the main influx of tidal energy is through the Luzon Strait. If you do not do this it is possible that your analytic model which is based on this assumption is not valid.

Reply: We calculated the tidal energy density of K₁ and 0.99 d⁻¹, and the results are shown in Figure 2b and 4b. See the R1 to be revised.

6. Line 72: Boundary Condition

More information is needed on the boundary of the model. The domain described in the text seems to be similar to Cui et al (2015) which makes me suspect you used the same code in the same configuration. However, the other paper shows a southern boundary south of the Equator, whereas according to your text the present one is north of the Equator. Why the difference?

Reply: In Cui et al. (2015), the southern boundary is set at 2°S, but in this paper, the southern boundary moves northward to 1.5°N. This change in the southern open boundary does not influence the resonant frequencies but slightly improves the patterns of the amplitude gain and phase change.

Figure 1, which the caption calls the study area, shows only part of the model domain. Why is this? When I first read the introduction and saw this figure, I assumed that this included the model domain with say Luzon Strait as an open boundary and the regions you described as having negligible fluxes as closed boundaries. Your need to make the difference clearer earlier in the paper.

Reply: In R1, we have included an inset in the upper-left corner in Figure 1 showing the entire model domain, and the figure caption is revised as follows: “The South China Sea and its neighbouring area. The contours show the water depth distribution in metres. The blue line B is the mouth cross section of the Gulf of Thailand (GOT). The triangles represent the tidal gauge stations (the full names of

these stations are given in Table 1). The inset in the upper-left corner shows the entire model domains (99-131°E, 1.5-42°N)".

You say that the northern and eastern boundaries are set well away from the South China Sea to limit the effect of the (fixed) boundary condition on the resonances of the South China Sea. However what about the boundaries to the south and east?

Reply: We add the following sentence: "The southern open boundary is set along a latitudinal section of 1.5 °N, which meets the southernmost tip of the Malay Peninsula".

6. Line 64 and 80-90: Real and complex variables

Analysis of waves and oscillating systems tends to be a lot neater and easier to understand when the physical wave is treated as the real part of a function of the type $A(x) \exp(-i \omega t)$ where A is a complex number and i is the complex i . Then your G and ϕ are just the amplitude and phase of a complex response function. The appendix would also be a lot shorter if you used complex variables whenever possible.

Reply: Since we use POM in the numerical computations, it is more direct and easier to understand to express the variables as usual functions of x , y and t in the sections on numerical modelling. In the section on theoretical model and in the appendix, we use complex variables as you suggested.

7. Lines 94-96

This is a bit of a mess and needs to be rewritten. From Cui et al. (2015) you know that there are resonant like features which affect both the Gulf of Thailand and the South China Sea. We know that if the Gulf of Thailand was removed, changing the depth of the South China Sea would affect its resonances. Thus what you are really doing here is to see how much changing these resonances affects the resonances of the combined system. (You could have also carried out runs with changed depths in the Gulf of Thailand - in fact I am surprised that you didn't).

What you are not doing here is finding out how the resonances of the South China Sea are affecting (i.e. changing the shape and frequency of) the localised resonances of the Gulf of Thailand.

Reply: According to your comment, we have carried out two additional experiments (numbered Exps. 4 and 5), in which the depths in the GOT are artificially multiplied by 1/2 and 2. The results are added to Table 2 and Figure 3 in R1.

8. Line 100- : The Results

The paper does not specify the geographical location used for figures 2a and 2b. The three SCSB peaks referred to in table 1 refer to the three main peaks of fig 2a. Changing the depth by a factor of 2 seems to change the frequencies by roughly $\sqrt{2}$, but this is not discussed.

Reply: (1) In the present study, we do not use specified locations to represent the area of concern; rather, we use the area-mean value of the top 20% amplitude gain to represent the amplitude gain of the corresponding area. This statement was given in the original manuscript and is retained in R1. For clarity, we added this statement to the captions of these figures in R1. (2) This is a good point; thank you. We added the following statement to R1: "It is worth noting that when the depths in the SCSB are artificially changed by factors of 1/2 and 2, the resonant frequencies are roughly changed by factors of $\sqrt{1/2}$ and $\sqrt{2}$, respectively. This indirectly indicates that the quarter-wavelength resonance theory is applicable to the SCS".

Exp 3 shows a second resonance near 1 cycle/day which also seems to have an effect in fig 2b. Changing the depth of the South China Sea will change the frequency of resonances but will not generate new ones. So what is this feature of the South China Sea affecting the Gulf of Thailand?

Reply: In Exp. 3, there is another weaker peak in the SCSB at the frequency of approximately 1.15 d^{-1}

(Figure 3a of R1). The peak frequency response may also have an effect on the GOT (plot for Exp. 3 in Figure 3b of R1), which results in a plateau peak of the GOT between 0.5 d^{-1} and 1.2 d^{-1} . We speculate that this is probably due to the fact that deepening the SCSB may result in a discontinuity of topographic data at the junction with the GOT. However, we are not sure of this speculation, and it is not included in R1.

In the case of fig 2b, representing the Gulf of Thailand response, there are indeed three main peaks matching the peaks in the South China sea plot - but there is also a lot else going on, especially in expt 1 and 2. What resonances are these?

Reply: The second peak of the GOT's response function at the frequency 0.45 d^{-1} is of some importance. We added the following statement to R1: "In addition, there is a weak response peak at the frequency 0.45 d^{-1} in the GOT (Exp. 1 in Figure 3b). Since the GOT has a length of 660 km and a mean depth of 36 m, the quarter-wavelength theory gives a resonant frequency of 0.61 d^{-1} . It seems that the peak at 0.45 d^{-1} is associated with the local regional resonance". Since in this part of study, we use real coastline and topography, which are irregular, the response function also contains some irregular fluctuations, which are difficult to explain.

It should help if the paper illustrated the amplitude and and phase of key resonances. The simplest solution would be to give the amplitude and phase of the solution when forced at the frequencies of the peaks in the response function. A better alternative would be to fit the (complex) response function $R(x, w)$ at a set of w 's around each of the resonance peaks to the equation $A(x)/(w-w_0) + B(x) + C(x)*(w-w_0)$ Where A, B, C, w_0 are complex, x is position, w is the (real) angular velocity of the forcing and w_0 the estimated (complex) angular velocity of the resonance. $A(x)$ would then be a better approximation to the amplitude and phase of the true resonance. Following the changes, the conclusions to this section need to be rewritten.

Reply: (1) According to this comment, we have added a figure on the distributions of amplitude gains and phase changes to R1 (as Figure 4a). (2) $A(x)/(w-w_0) + B(x) + C(x)*(w-w_0)$ is a useful equation. Similar equations have been successfully applied to various sea areas to estimate resonant frequency and quality factor Q (e.g., Garrett and Munk, 1971, The age of the tide and the Q of the oceans, DSR; Sutherland et al., 2005, Tidal resonance in Juan de Fuca Strait and the Strait of Georgia, JPO). However, this or similar equations are generally used to fit the observed responses due to sparse sampling in terms of spectrum resolution. For example, in a semidiurnal band, only responses at frequencies of N_2 , M_2 , S_2 and K_2 are generally available. In the present study, the response functions are numerically generated. They are smooth and have fine resolution. Hence, fitting by the above equation would not yield significantly different results. The corresponding author (G. Fang) plans to use this equation in a future study.

9. Line 128

Semantics - the theory is 'applicable' to the Gulf of Thailand but does not explain the enhanced tides around 1 cycle day (although it might explain an enhancement if forced at 2 cycles/day).

Reply: Revised as suggested (the observation shows that semi-diurnal tides are small).

10. Lines 147-160

It would be best if most of this was kept in the appendix. All you really need is eqn 15 and the approximation when $r*p_1/p_2$ is small.

Reply: Most of the equations have been removed as suggested.

11. Lines 165-185.

I think this needs a little more thought. You should be able to show that the resonances near 0.5 and 2

cycles per day are resonances of the short channel (where $\cos(\beta_2 L_2)$ is zero) and the one near 1 cycle per day is a resonance of the long channel (where $\cos(\beta_1 L_1)$ is zero). Then friction reduces the amplitude of the shallow short channel resonances but has little effect on the amplitude of the long channel resonances except within the shallow channel.

Reply: According to your comment, we have added the following paragraph: “If we apply the quarter-wavelength resonance theory to channel 1, we can obtain resonant frequencies of 0.99 d^{-1} . If we apply the quarter-wavelength and three-quarter-wavelength resonance theories to channel 2 we can obtain resonant frequencies of 0.61 and 1.84 d^{-1} , respectively. Therefore, we can conclude that the major peaks around the frequency of 1.04 d^{-1} in Figure 6 are caused by resonance in channel 1. This indicates that channel 1 plays a determinative role in the two-channel system. Similarly, we can also conclude that the secondary and third peaks around the frequencies of 0.55 and 1.85 d^{-1} in Figure 6 are caused by resonances in channel 2, associated with the quarter-wavelength and three-quarter-wavelength resonances. Although the frequencies of the peaks shown in Figure 6 correspond well with those estimated based on the quarter-wavelength and three-quarter-wavelength theories, there are small discrepancies. This is due to the connection of the two channels. In fact, the resonant frequencies of the two-channel system also depend on the depth ratio of two channels, as shown in Eq. (14). In comparison to channel 2, the secondary, especially the third peak, in channel 1 is much more less significant. This can be explained as follows: The tidal incident wave from the channel 1 partially enters channel 2 across the steep topography at $x = 0$, and here, the rest of the wave is reflected. The reflected wave is superimposed with the incident wave, and tidal resonance occurs around the frequency of 1.04 d^{-1} . That is, the steep topography at $x = 0$ acts as a wall for channel 1, which causes the quarter-wavelength resonance to occur in the channel. Furthermore, the steep topography can also block most energy of the wave in channel 2 from entering channel 1. Therefore, the relatively large amplitudes in channel 2 at frequencies around 0.55 d^{-1} and 1.85 d^{-1} are not obvious in channel 1 under the action of friction”.

12. Lines 189-195

I suppose my main point here is that the diurnal resonance affecting the Gulf of Thailand is not 'closely related' to that affecting the South China Sea. Instead it is exactly the same resonance.

Reply: Revised as suggested. The statement is changed to “Changing the water depths in the SCSB in our numerical experiments further shows that the resonance of the SCSB has a critical impact on the resonance of the GOT”.

13. Appendix

This seems a bit long for the content. I suggest that you cut it down in size, trying to make it more elegant and leaving out some of the obvious steps.

Reply: We simplified the appendix as suggested. Nearly 2/3 of the equations have been removed.

Modification list

(According to Revision #1-Updated manuscript)

Page 1.

In the abstract, we have accepted the suggestion of Dr. Webb.

Lines 7-10. The word “period” or “periods” has been replaced with “frequency” or “frequencies”, and the corresponding “one day” has also been replaced with “one cycle per day”. The words “is approximately” have been replaced with “has a strong response”.

Lines 13-16. We have added this sentence “We find that the resonant frequency ... the main area of the South China Sea”.

Line 20. Because Figure 1 was replaced with a new figure, the word “red” was changed to “blue”.

Page 2.

Lines 2-5 and line 13. The word “period” or “periods” has been replaced with “frequency” or “frequencies”, and the corresponding number has also been changed.

Lines 20-21. We have agreed with Dr Webb, so “... the resonant period in the GOT ... and SCSB are closely related” has been replaced with ‘... the GOT to have a strong response... both the SCSB and the GOT.’

Line 22. Because the content in section 2 has been changed and we have added section 2.2, the title of section 2 “Numerical methods for estimating the resonant frequency” has been replaced with “The numerical model”.

Line 23. The title of section 2.1 “Governing equations” has been replaced with “Governing equations and model configuration”.

Lines 24-25. We have accepted the suggestion of Dr Webb, so we have added the sentence “In this paper, we use the Princeton Ocean Model (POM) for numerical investigation, but we partially modify its code to meet the needs of the present study”.

Line 32. We added the reference “Webb, 2014”.

Page 3

Lines 7-11. We have added the content of the model configuration. “The computational domain selected is in the range of 99-131 °E and of 1.5-42 °N. ... data extracted from navigational charts.’

Lines 12-28. We accept the suggestion of Dr Webb, so we newly added section 2.2 about the simulation of the K₁ tide. For details, please see section 2.2 of Revision #1.

Page 4.

Line 1. We have added a new title “3 Numerical methods for estimating the resonant frequency”.

Lines 12-14. Since the part of the model configuration have already existed in Page 3 lines 7-11, we

deleted it here, and we have added “Through the simulation of the K_1 tide ... values at the open boundaries are changed as follows”, which makes the context more coherent.

Pages 5-6. Section 4

In section 4, we have accepted the suggestion of Dr Webb, and this section has been almost rewritten.

Page 5. Lines 6-10. We have added this new paragraph “Cui et al. (2015) revealed that both the SCS ... be related to the SCS resonance.”, which explains why we studied the influence of resonance in South China Sea on the Gulf of Thailand.

Page 5. Lines 11-16. Since we have carried out two additional experiments 4-5 (numbered Exps. 4 and 5), we added the sentence “In Exp. 4 and 5, we change... SCSB retains the real depths”.

Page 5. Lines 16-18. In order to express the experimental results more clearly, we have accepted the suggestion of Dr. Webb, and we have added this sentence “The results of these six experiments are shown ... peak responses are listed in Table 2.”

Page 5. Lines 19-25. This paragraph was newly added. In this paragraph, we compared the spatial patterns of 0.99 d^{-1} and K_1 to show that the experimental method is feasible. “Table 2 and Figure 3 show that when real water depths are used ... Minor differences are caused by the use of different open boundary conditions.”

Page 6. Lines 1-3. We have accepted the suggestion of Dr Webb, and we have added the analysis “It is worth noting ... theory is applicable to the SCSB.”.

Page 6. Lines 5-7. In these lines, we explained the reasons of producing 1.15 d^{-1} in Exp.3, but we were not sure of the speculation. The details are “The peak frequency response ... at the junction with the GOT”.

Page 6. Lines 9-13. Since we have carried out two additional experiments (Exps. 4-5), we added this new paragraph. The details are “Experiments 1-3 suggest that ... are still close to one cycle per day”.

Page 6. Lines 14-15. We have rewritten the lines. “In this experiment, the boundary ... as shown in Fig. 3” have been replaced with “In Exp. 6, the mouth boundary ... as shown in Fig. 3c”.

Page 6. Lines 21-24. We have added these new lines to explain the reason of producing 0.45 d^{-1} in Exp. 1. The details are “In addition, there is a weak ... associated with the local regional resonance.”

Page 6. Lines 25-29. This paragraph is the summary of section 4, and we have moved the summary to the end of section 4.

Page 6.

Lines 31-32. We have accepted the suggestion of Dr. Webb, the sentence “this theory is not applicable to the GOT” has been replaced with “this theory does not explain the enhanced tides around one cycle per day in the GOT.”

Page 7.

Lines 4-5. We have added the new sentence “This model is quite similar to Webb’s (2011) 1-D model, except that we add a forcing at the entrance of the deep channel”.

Lines 16-17. We have added the new sentence “By eliminating the common ... equations as follow” to make the context coherent.

Page 8.

Lines 5-10. We have accepted the suggestion of Dr. Webb, and we have deleted some equations which have existed in appendix. Besides, we have added the new sentence “When the denominator ... in Appendix (Eq. A10):” to make enunciated coherent

Page 9.

Lines 1-16. We have accepted the suggestion of Dr. Webb. We have added the new paragraph about the further analysis of the theoretical model results. For details, please see Page 9, lines 1-16.

Lines 29-30. “... that the resonance of the GOT is closely related to the resonance in the SCSB” has been replaced with “... that the resonance of the SCSB has a critical impact on the resonance of the GOT”

Page 9, line 31-page 10, line 2.

We have added the new sentence “Through the numerical experiments and two-channel model ... the main area of the South China Sea”

Page 10

Line 9. Since we have added the content about simulation of K_1 tide which needs the data of the open boundaries, we added the line “The tidal data at the open boundaries are available online at <ftp://ftp.oce.orst.edu/dist/tides>.”

Page 10, line 10-page 12, line 13.

This section is the appendix. In this section, we also have accepted the suggestion of Dr. Webb, and we have simplified the appendix. Nearly 2/3 of the equations have been removed.

Page 13

Lines 4-7. We sincerely thank the topic editor and two referees, and we have added these words “The authors sincerely thank the topic editor ... were of great help in improving our study.”

Line 15. We have added the reference “Egbert G D, Erofeeva S Y...” which is referenced on page 3, line 15.

Page 14

Lines 3-5. We added two references of Dr Webb, which were of great help and were referenced on Page

3, line 28 and page 7, line 4, respectively.

Page 15

Lines 2-4. Figure 1 which is on page 20 has been replaced with the new picture, so the caption was changed to “The South China Sea ... domains (99-131°E, 1.5-42°N)”

Lines 5-6. Figure 2 which is on page 21 was the newly added picture. The caption “Figure 2: Model-produced ... flux density vectors (in kW m⁻¹).”

Lines 8-9. Figure 3 has been replaced with the new one which is on page 22, and in the caption, we newly have added the sentence “Here, the amplitude gains ... given in Table 2” which makes the meaning of Figure 3 clear.

Lines 10-11. Figure 4 which is on page 22 was the newly added picture. The caption “Figure 4: (a) Distribution ... flux density vectors.”

Pages 16-17.

Table 1 was the newly added table. For details, please see page 16-17.

Page 18

Table 2 has been updated because we have carried out two additional experiments. For details, please see page 18.

Revision #1 - an updated manuscript

Tidal resonance in the Gulf of Thailand

Xinmei Cui^{1,2}, Guohong Fang^{1,2}, Di Wu^{1,2}

¹First Institute of Oceanography, Ministry of Natural Resources, Qingdao, 266061, China

²Laboratory for Regional Oceanography and Numerical Modelling, Qingdao National Laboratory for Marine Science and Technology, Qingdao, 266237, China

Correspondence: Guohong Fang (fanggh@fio.org.cn)

Abstract. The Gulf of Thailand is dominated by diurnal tides, which indicates that the resonant frequency of the gulf is close to one cycle per day. However, when applied to the gulf, the classic quarter-wavelength resonance theory fails to yield a diurnal resonant frequency. In this study, we first perform a series of numerical experiments showing that the gulf has a strong response near one cycle per day and that the resonance of the South China Sea main area has a critical impact on the resonance of the gulf. In contrast, the Gulf of Thailand has little influence on the resonance of the South China Sea main area. An idealised two-channel model that can reasonably explain the dynamics of the tidal resonance in the Gulf of Thailand is then established in this study. We find that the resonant frequency around one cycle per day in the main area of the South China Sea can be explained with the quarter-wavelength resonance theory, and the large-amplitude response at this frequency in the Gulf of Thailand is basically a passive response of the gulf to the increased amplitude of the wave in the southern portion of the main area of the South China Sea.

1 Introduction

The Gulf of Thailand (GOT) is an arm of the South China Sea (SCS), the largest marginal sea of the western Pacific Ocean (Fig. 1). The width of the GOT is approximately 500 km, and the length of the GOT from the top to the mouth of the gulf, as indicated by the blue line B in Fig. 1, is approximately 660 km. The mean depth in this area is 36 m according to the ETOPO1 depth data set (from the US National Geophysical Center). The mean depth of the SCS from the southern opening of the Taiwan Strait to the cross section at 1.5°N is 1323 m. If the GOT is excluded, the mean depth of the rest of the SCS (herein called the SCS body and abbreviated as SCSB) is 1457 m. Tidal waves propagate into the SCS from the Pacific Ocean through the Luzon Strait (LS) and mainly propagate in the southwest direction towards the Karimata Strait, with two branches that propagate northwestward and enter the Gulf of Tonkin and the GOT. The energy fluxes through the Mindoro and Balabac Straits are negligible (Fang et al., 1999; Zu et al., 2008; Teng et al., 2013). The GOT is dominated by diurnal tides, and the strongest tidal constituent is K_1 (Aungsakul et al., 2011; Wu et al., 2015).

The resonant responses of the GOT to tidal and storm forcing have attracted extensive research interest. However, the previous results have been diverse. Yanagi and Takao (1998) simplified the GOT and Sunda Shelf as an L-shaped basin and concluded that this basin has a resonant frequency near the semi-diurnal tidal frequency. Sirisup and Kitamoto (2012)

Deleted: period

Deleted: potentially

Deleted:

Deleted: t

Deleted: give

Deleted: period

Deleted: resonant period of

Deleted: the

Deleted: is approximately

Deleted: body

Deleted: the resonance of

Deleted: body

Deleted: red

applied a normal mode decomposition solver to the GOT and Sunda Shelf area and obtained four eigenmodes with modal frequencies of 0.42, 1.20, 1.54 and 1.76 d⁻¹ (cycle per day). Tomkratoke et al. (2015) further studied the characteristics of these modes and concluded that the mode with a frequency of 1.20 d⁻¹ is the most important. Cui et al. (2015) used a numerical method to estimate the resonant frequencies of the seas adjacent to China, including the SCS and the GOT, and found that the GOT has a major resonant frequency of 1.01 d⁻¹ and a minor peak response frequency of 0.42 d⁻¹. In these studies, except for Yanagi and Takao (1998), no effort was made to establish a theoretical model of the GOT, and the resonant period estimated by Yanagi and Takao (1998) cannot be used to explain the resonance of the diurnal tides.

The GOT is a semi-enclosed gulf with an amphidromic point in the basin for each K₁ and O₁ constituent. Wu et al. (2013) reproduced the tidal system well with superimposed incident and reflected Kelvin waves and a series of Poincare modes. This result raises the question of whether the quarter-wavelength resonant theory can explain the tidal resonance in the gulf, as is the case with other areas (Miles and Munk, 1961; Garrett, 1972; Sutherland et al., 2005). According to quarter-wavelength theory, because the distance from the head of the gulf to the mouth is approximately 660 km and the mean depth is approximately 36 m, the resonant frequency should be 0.61 d⁻¹, which is much lower than the estimates by Cui et al. (2015) and Tomkratoke et al. (2015). Thus, it is clear that the tidal resonance phenomenon in the GOT cannot be reasonably explained by the quarter-wavelength theory.

According to the theories of Garrett (1972) and Miles and Munk (1961), tidal oscillations are limited to a specific area. In contrast, Godin (1993) proposed that tides are a global phenomenon that cannot be separated into independent subdomains. The GOT is an auxiliary area of the SCS and is connected to the SCSB. We thus believe that Godin's theory is applicable to the GOT. In this paper, by considering the bathymetry of the SCSB in numerical experiments and theoretical analyses, we investigate the reasons for the GOT to have a strong response around the frequency of one cycle per day and how the physical properties of the SCSB primarily determine the resonances of both the SCSB and the GOT.

2 The numerical model

2.1 Governing equations and model configuration

In this paper, we use the Princeton Ocean Model (POM) for numerical investigation, but we partially modify its code to meet the needs of the present study. This study is limited to the main mechanism of diurnal tidal resonance; accordingly, the elimination of tidal forces and nonlinear terms and the linearisation of bottom friction in the control equation will not affect the problem we are studying, and the two-dimensional model effectively suits our purpose as shown in a number of previous studies (e.g., Garrett, 1972; Godin, 1993; Webb, 2014; Cui et al., 2015). The general forms of the equation of continuity and the equation of motion used in this study are as follows:

$$\frac{\partial \tilde{\zeta}}{\partial t} = -\frac{1}{R \cos \varphi} \left[\frac{\partial(H\tilde{u})}{\partial \lambda} + \frac{\partial(H\tilde{v} \cos \varphi)}{\partial \varphi} \right], \quad (1)$$

Deleted: periods

Deleted: 56.61

Deleted: 20.05

Deleted: 15.60

Deleted: 13.64

Deleted: h

Deleted: period

Deleted: 20.05

Deleted: h

Deleted: periods

Deleted: period

Deleted: 23.8

Deleted: h

Deleted: period

Deleted: 59.9

Deleted: h

Deleted:

Deleted:

Deleted: period

Deleted: 39.04 h

Deleted: long

Deleted:

Deleted: .

Deleted: w

Deleted: why

Deleted: the resonant period in the GOT produces an approximately diurnal tide and why the resonant periods of the GOT and SCSB are closely related

Deleted: Numerical methods for estimating the resonant frequency

Deleted: 2.1 Governing equations

Deleted: and does not intend to simulate the tides;

Deleted: continuity

Deleted: motion

$$\frac{\partial \tilde{u}}{\partial t} = 2\Omega \tilde{v} \sin \phi - \frac{g}{R \cos \phi} \frac{\partial \tilde{\zeta}}{\partial \lambda} - \frac{\tau \tilde{u}}{H}, \quad (2)$$

$$\frac{\partial \tilde{v}}{\partial t} = -2\Omega \tilde{u} \sin \phi - \frac{g}{R} \frac{\partial \tilde{\zeta}}{\partial \phi} - \frac{\tau \tilde{v}}{H}, \quad (3)$$

where t denotes time; λ and ϕ , respectively, refer to the east longitude and north latitude; $\tilde{\zeta}$ is the surface height above the undisturbed sea level; \tilde{u} and \tilde{v} represent the east and north components of the fluid velocity, respectively; R indicates the Earth's radius; Ω refers to the angular speed of the Earth's rotation; g is the gravitational acceleration; H denotes the undisturbed water depth; and τ represents the linearised bottom friction coefficient.

The computational domain selected is in the range of 99-131 °E and of 1.5-42 °N. The northern and eastern open boundaries are located far beyond the area of the SCS to prevent the numerical values at the open boundaries from influencing the results in the study area. The southern open boundary is set along a zonal section of 1.5 °N, which meets the southernmost tip of the Malay Peninsula. The grid resolution is 1/12°. The water depths are basically taken from the ETOPO1 data set and are modified using depth data extracted from navigational charts.

2.2 Simulation of the K₁ tide

To examine the applicability of the modified POM model to the study area, the model is first used to simulate the K₁ tide in the SCS and its neighbouring area. The amplitudes and phase-lags along the open boundary are taken from the global tidal model TPXO9, which is based on satellite altimeter observations (Egbert and Erofeeva, 2002). The model-produced K₁ tidal system is shown in Figure 2a, and a comparison of the model results with observations at 31 tidal gauge stations is shown in Table 1. The locations of these tidal stations are shown in Figure 1, from which it can be seen that the stations are basically evenly distributed along the coast of the SCSB and GOT.

From Table 1, we can see that the deviations in amplitudes are mostly within 0.05 m, while those in phase-lags are mostly within 20°. Considering that the governing equations are greatly simplified, the linearised bottom friction is used to replace the more accurate quadratic form, the agreement between model results and observations can be regarded as satisfactory. Therefore, the modified model is applicable to the SCS and GOT tidal study.

To show the characteristics of the wave propagation process, we calculate the tidal energy flux density distribution, as given in Figure 2b. One can see that the K₁ tidal wave mainly enters the SCS through the LS and spreads southward, partially moves to the GOT, and partially exits the SCS through the Karimata Strait. Figure 2a shows that the K₁ tidal amplitudes are large in the Gulf of Tonkin and that there is an amphidromic point at the mouth of the gulf caused by one-quarter wavelength resonance (Fang et al., 1999). In the GOT, there is also an amphidromic point, but away from the mouth section, indicating that the amplified K₁ tide cannot be attributed to the quarter-wavelength resonance.

Deleted: .

Deleted: z

3 Numerical methods for estimating the resonant frequency

3.1 Open boundary condition

The open boundary condition for the tidal resonant study can be written in the following form:

$$\tilde{\zeta}(i, j, t) = \sum_{n=N_1}^{N_2} \tilde{Z}_n(i, j) \cos[2\pi f_n t - \tilde{\theta}_n(i, j)], \quad (4)$$

- 5 where (i, j) are grid points on the open boundary; $f_n = n\Delta f$ refers to the frequency of the n -th wave of interest, with Δf referring to the spectrum resolution; and for $n = N_1, N_1 + 1, \dots, N_2$, \tilde{Z}_n and $\tilde{\theta}_n$ represent the amplitude and phase lag of the n -th wave, respectively. In this study we choose $\Delta f = 1/1024 \text{ h}^{-1}$ for the following two reasons: First, the value 1024 is equal to 2^{10} , enabling us to efficiently calculate spectra from model-produced time series by using a fast Fourier transform (FFT). Second, because the minimum frequency difference between the main tidal constituents (Q_1 , O_1 , K_1 , N_2 , M_2 , and S_2) is equal to $1.51 \times 10^{-3} \text{ h}^{-1}$, the resolution of $\Delta f = 1/1024 \text{ h}^{-1}$ is sufficient for separating these constituents.

3.2 Numerical model of the seas adjacent to China

Through the simulation of the K_1 tide, it is shown that the modified model can be applied to tidal study. The model setting is consistent with the setting of the simulation of the K_1 tide except that the water level values at the open boundaries are changed as follows. The amplitudes \tilde{Z}_n at the open boundaries are specified as a constant, 2 cm; the phase-lags $\tilde{\theta}_n$ are

- 15 given as random numbers that are evenly distributed in the interval $(0, 2\pi)$ and generated using a normal random number generator. The purpose of using random phase lags is to avoid all or some of the waves to have the same phase at a certain time, which can lead to simultaneous unreasonably high or low sea levels. The selected N_1 and N_2 values are 1 and 107, respectively. Thus, the frequencies of the waves studied range from $1/1024$ - $107/1024 \text{ h}^{-1}$ or 0.0234 - 2.5078 d^{-1} . The corresponding periods range from 10 - 1024 h (approximately 0.4 - 42.7 days), which covers all main tidal constituents.

- 20 In the last cycle of 1024 hours, the hourly results at each grid point are preserved, and FFT analysis is performed to yield amplitude Z_n and phase lag θ_n . The amplitude ratio is defined as follows:

$$G_n = Z_n / \tilde{Z}_n, \quad (5)$$

and the phase lag difference is given by the following equation:

$$\psi_n = \theta_n - \tilde{\theta}_n. \quad (6)$$

Deleted: 2.2

Field Code Changed

Deleted: $\tilde{\zeta} = \text{Re} \left(\sum_{n=N_1}^{N_2} \tilde{Z}_n e^{i[2\pi f_n t - \tilde{\theta}_n]} \right)$

Deleted:

Deleted:

Deleted: e

Deleted: 2.3

Deleted: The computational domain selected is in the range of 99-131 °E and of 1.5-42 °N. The northern and eastern open boundaries are chosen to locate far beyond the area of the SCS to prevent the numerical values at the open boundaries from influencing the results in the study area. The grid resolution is 1/12°. The water depths are basically taken from the ETOPO1 data set and are modified using depth data extracted from navigational charts.

Deleted: ay

Deleted: (cycles per day)

Deleted: 9

Deleted: 3

Deleted: frequencies

Deleted: , where (i, j) denotes a grid point in the inner computational domain

According to Munk and Cartwright (1966), $Ge^{-i\psi}$ is the admittance. Specifically, as Munk and Cartwright (1966) stated, G_n is the amplitude response and represents the amplification factor of the n -th wave in response to forcing. In the present study, we call G_n and ψ_n the amplitude gain and phase change, respectively, in accordance with Sutherland et al. (2005) and Roos et al. (2011).

Deleted: at point (i, j) ...in response to forcing. In the present ...

5 4 Influence of resonance in the main area of the South China Sea on the Gulf of Thailand

Deleted: 5 Influence of resonance in the main area of the Sou...

Cui et al. (2015) revealed that both the SCS and GOT have strong response peaks around one cycle per day and suggested that the resonance of the SCS could be explained by one-quarter wavelength resonance theory, but the authors did not provide the reasons for the strong response of the GOT around this frequency. As an arm of the SCS, the tidal energy of the GOT comes mainly from the SCSB (Figure 2b), so we speculate that the strong response of the GOT around one cycle per day may be related to the SCS resonance.

To examine the influence of SCSB resonance on GOT, we conduct six numerical experiments: Exp. 1 to Exp. 6. In Exp. 1, we use real bottom topography. In Exp. 2, we artificially make the depths in the SCSB equal to half of the real depths and retain the depths in the GOT. In Exp. 3, the depths in the SCSB are artificially doubled and the depths in the GOT remain unchanged. In Exp. 4 and 5, we change the water depths of the GOT by factors of 1/2 and 2, respectively, and the SCSB depths remain unchanged. In Exp. 6, the mouth boundary of the GOT (indicated by the blue line B in Fig. 1) is artificially closed and the SCSB retains the real depths. The results of these six experiments are shown in Figure 3, in which the area-mean values of the top 20% amplitude gains are used to represent the response of the corresponding area. The resonant frequencies corresponding to peak responses are listed in Table 2.

Deleted: resonance, we conducted ...sixthree...numerical ...

Table 2 and Figure 3 show that when real water depths are used, the resonant frequency of the SCSB appears at 0.99 d^{-1} while that of the GOT is 1.01 d^{-1} . The resonant frequencies of these two areas are basically the same, and both are very close to that of the diurnal tide K_1 , whose frequency is equal to 1.00 d^{-1} (or more precisely, 1.0027 d^{-1}). The spatial patterns of the amplitude gain and phase change for the frequency 0.99 d^{-1} are displayed in Figure 4a, with corresponding energy flux density vectors shown in Figure 4b (the corresponding figures for 1.01 d^{-1} are almost the same and are thus not shown). We can find that the patterns shown in Figure 4 are quite similar to the simulated K_1 patterns shown in Figure 2. Minor differences are caused by the use of different open boundary conditions.

Deleted: 1 and Figure 3. 2...show that when real water depths ar...

From Figures 3a and 3b, we can see that the peak amplitude gains in the GOT and SCSB are reduced when the depths of the SCSB are changed to half of the real depths. This reduction in amplitude gain occurs because friction increases as depth decreases (see Eqs. (2) and (3)). Moreover, the amplitude peak frequencies in the GOT and SCSB both change to 0.75 d^{-1} (Figure 3a-b and Table 2), indicating that the resonant frequency in the GOT is determined by that of the SCSB. When the depths of the SCSB are doubled, the amplitude peak frequencies of the SCSB and GOT are increased to 1.49 and 1.50 , respectively (Figure 3a-b and Table 2), again indicating that the peak frequency of the GOT is determined by that of the

Deleted: , respectively, when real water depths are used. The resonant periods of the two areas are roughly the same, and both are close to the period of the diurnal tide K_1T...e peak amplitude ...

SCSB. It is worth noting that when the depths in the SCSB are artificially changed by factors of 1/2 and 2, the resonant frequencies are roughly changed by factors of $\sqrt{1/2}$ and $\sqrt{2}$, respectively. This indirectly indicates that the quarter-wavelength resonance theory is applicable to the SCSB.

In Exp. 3, there is another weaker peak in the SCSB at the frequency of approximately 1.15 d^{-1} (Fig. 3a). The peak frequency response may also have an effect on the GOT (Fig. 4b, Exp. 3), which results in a plateau peak of GOT between 0.5 d^{-1} and 1.2 d^{-1} . This may be due to the deepening of the SCSB, resulting in discontinuity of topographic data at the junction with the GOT. Moreover, the amplitude gains in the GOT are significantly increased by increasing the depth, which results in reduced friction (see Eqs. (2) and (3)).

Experiments 1-3 suggest that the peak response frequency of the GOT is strongly affected by the SCSB. Here, we conduct further experiments (Exps. 4-6) to investigate whether the GOT can also influence the resonance of the SCSB. From the results of Exps. 4-5 (Table 2, Figures 3c-d), it can be seen that changing the depths of the GOT has little effect on the peak response frequencies of the SCSB and GOT. That is, the resonant frequencies of both areas are still close to one cycle per day.

In Exp. 6, the mouth boundary of the GOT (indicated by the blue line B in Figure 1) is artificially closed. The results of this experiment show that the GOT has a small influence on the response of the SCSB, as shown in Fig. 3c. When boundary B is closed, the resonant frequency of the SCSB becomes slightly higher than the frequency of the K_1 tide, and the response amplitude of the SCSB in the vicinity of the resonant frequency is slightly reduced. As indicated by Arbic et al. (2009), when a shallow basin is connected to a deep basin, the impact of the shallow basin on the tidal response in the deep basin is determined by the depth ratio, width ratio, and length ratio of these two basins, as well as the friction in the shallow basin. In the present case, the depth and width ratios of the GOT against the SCSB are small, and tides in the GOT are strongly damped, so the impact of the GOT on the SCSB is not significant. In addition, there is a weak response peak at the frequency 0.45 d^{-1} in the GOT (Exp. 1 in Figure 3b). Since the GOT has a length of 660 km and a mean depth of 36 m, the quarter-wavelength theory gives a resonant frequency of 0.61 d^{-1} . It seems that the peak at 0.45 d^{-1} is associated with the local regional resonance.

In summary, the resonant periods or frequencies change when the depth of the SCSB varies, and the trends in the two sea areas are consistent (Figure 3). The resonant frequency decreases when the SCSB is shallower and increases when the SCSB is deeper. Additionally, the resonant frequencies of the SCSB and GOT remain almost identical (Table 2). The experimental results show that the SCSB has a critical impact on the tidal resonance of the GOT and that the GOT is not an independent sea area in terms of tidal resonance.

5. A theoretical model

The quarter-wavelength resonant theory is based on the wave behaviour in a single channel. As discussed above, this theory does not explain the enhanced tides around one cycle per day in the GOT. Here, we establish a two-channel model and

Deleted: 2

Deleted: :

Deleted: this result might be caused by the use of two times the real depth in the SCSB, and the SCSB is deeper than the LS.

Deleted: In summary, the resonant periods or frequencies change when the depth of the SCSB varies, and the trends in the two sea areas are consistent (Fig. 2). The resonant frequency decreases when the SCSB is shallower and increases when the SCSB is deeper. Additionally, the resonant frequencies of the SCSB and GOT remain almost identical (Table 1). The experimental results show that the SCSB has a critical impact on the tidal resonance of the GOT and that the GOT is not an independent sea area in terms of tidal resonance. .

Deleted: The above experiments suggest that the tidal resonance in the GOT is strongly affected by the SCSB, the main part of the SCS. Here, we conduct an additional numerical experiment to investigate whether the GOT can also influence the resonance of the SCSB. In this experiment, the boundary of the GOT (indicated by the red line B in Fig. 1) is artificially closed, and the response function of the SCSB is examined. The results show that the GOT has a small influence on the response of the SCSB, as shown in Fig. 3.

Deleted: ,

Deleted: in

Deleted: .

Deleted: 6

Deleted:

Deleted: mentioned

Deleted: is

Deleted: applicable to

examine its applicability to the SCSB-GOT system. Tidal waves from the Pacific Ocean propagate through the LS, pass the SCSB and finally enter the GOT. The tidal waves in the Karimata Strait are very weak (Figure 2a and Wei et al., 2016) and are not able to propagate into the GOT. Thus, the tidal energy in the GOT is mainly from the SCSB. Therefore, we use a two-channel model to represent the SCSB-GOT system, as shown in Fig. 5. This model is quite similar to Webb's (2011) 1-

5 D model, except that we add a forcing at the entrance of the deep channel. In the figure, H_1 is the depth of channel 1 (the deep channel), H_2 is the depth of channel 2 (the shallow channel), and L_1 and L_2 are the lengths of channels 1 and 2, respectively. The tidal waves enter channel 1 through the opening at $x = L_1$, enter channel 2 through the junction point at $x = 0$, and finally reach the top of channel 2 at $x = -L_2$. The equations governing the tidal motion in channels can be expressed as follows:

$$10 \quad \begin{cases} \frac{\partial \tilde{u}_m}{\partial t} = -g \frac{\partial \tilde{\zeta}_m}{\partial x} - \gamma_m \tilde{u}_m \\ \frac{\partial \tilde{\zeta}_m}{\partial t} = -H_m \frac{\partial \tilde{u}_m}{\partial x} \end{cases}, \quad (7)$$

where $\tilde{\zeta}_m(x, t)$ and $\tilde{u}_m(x, t)$ represent the elevation and velocity, respectively; H_m is the depth; γ_m is the friction parameter (equivalent to τ/H in Eqs. (2) and (3)); g is the acceleration due to gravity; and $m = 1, 2$ represents the different channel segments. Here, $\tilde{u}_m(x, t)$ and $\tilde{\zeta}_m(x, t)$ can be expressed in the forms of $u_m(x, t) = \text{Re}(u_m(x) e^{-i\omega t})$ and $\zeta_m(x, t) = \text{Re}(\zeta_m(x) e^{-i\omega t})$, respectively, where ω is the angular frequency, t is time, and $\zeta_m(x)$ and $u_m(x)$ represent the complex amplitudes of the elevation and velocity, respectively. By eliminating the common factor $e^{-i\omega t}$, Eq.

(7) can be reduced to ordinary differential equations as follows:

$$15 \quad \begin{cases} -i\omega u_m = -g \frac{d\zeta_m}{dx} - \gamma_m u_m \\ -i\omega \zeta_m = -H_m \frac{du_m}{dx} \end{cases}. \quad (8)$$

The boundary and matching conditions are as follows:

$$\zeta_1(L_1) = a_0, \quad \zeta_1(0) = \zeta_2(0),$$

$$H_1 u_1(0) = H_2 u_2(0), \text{ and}$$

$$u_2(-L_2) = 0.$$

Deleted: 4

Field Code Changed

Field Code Changed

(9) Deleted: 8

(10) Deleted: 9

(11) Deleted: 0

From the governing equations and boundary/matching conditions, the complex amplitudes of the elevations of the two channels can be obtained as follows (see the appendix for a detailed derivation):

$$\zeta_1(x) = a_0 R_0 Q(x), \text{ and} \quad (12)$$

$$\zeta_2(x) = a_0 R_0 \cos \beta_2 (x + L_2). \quad (13)$$

5 When the denominator of R_0 reaches its minimum, the amplitudes of the two-sea area become the largest and resonance occurs. The condition is as follows (see expression of R_0 in Appendix (Eq. A10)):

$$|\cos \beta_1 L_1 \cos \beta_2 L_2 - r \frac{p_1}{p_2} \sin \beta_1 L_1 \sin \beta_2 L_2| = \min, \quad (14)$$

where $r = \sqrt{H_2/H_1}$.

Based on the configurations of the SCSB and GOT, we take $L_1 = 2600$ km, $L_2 = 660$ km, $H_1 = 1457$ m,

10 $H_2 = 36$ m, and $\gamma_m = \frac{0.0001}{H_m}$. By substituting these values into (12) and (13), we can obtain the solutions of these

equations. The amplitude gains at locations $x=0$ and $-L_2$ are functions of ω or functions of the frequency f ($f = \omega/2\pi$) and can be used to represent the response properties of channels 1 and 2, respectively. The results are shown with red curves in Figure 6. For comparison, we also calculate the corresponding functions in the absence of friction, as shown by the blue curves in Figure 6. From these curves, the resonant frequencies can be readily obtained, as given in Table

15 3.

Figure 6a displays the response function at $x = -L_2$, which represents the response of channel 2. This figure shows that the results in the presence of friction are more realistic than those in the absence of friction. The former case has a maximum peak at a frequency of 1.040 d^{-1} . The corresponding resonant period is 23.08 h, and this value is similar to the result of the numerical experiment involving the natural basin (Table 2, Exp. 1). The secondary response peak appears at a frequency of 0.558 d^{-1} , which is also fairly consistent with the results for the natural basin, as shown in Fig. 3b (red curve). The third peak is very small and appears at a frequency of 1.848 d^{-1} . If we carefully examine the red curve in Fig. 3b, we can also find a small peak near a frequency of 1.9 d^{-1} . The response function is worse when friction is neglected than when friction is retained, but the obtained resonant frequencies are almost unchanged, as shown by the blue curve in Figure 6a. Figure 6b shows the response function at $x = 0$, which represents the response of channel 1. The red curve has only one peak at a frequency of 1.040 d^{-1} , which is also similar to the results of the numerical experiment applied to the natural basin (Table 2, Exp. 1). When the friction is neglected, the frequency of the main peak is unchanged. In addition, there are two other peaks that are very narrow, indicating that these two peaks are relatively insignificant.

Deleted: A

Deleted: 1

Deleted: 2

Deleted: where .

$$R_0 = \frac{1}{\cos \beta_1 L_1 \cos \beta_2 L_2 - r \frac{p_1}{p_2} \sin \beta_1 L_1 \sin \beta_2 L_2},$$

and * * * (13) .

$$Q(x) = \cos \beta_1 x \cos \beta_2 L_2 - r \frac{p_1}{p_2} \sin \beta_1 x \sin \beta_2 L_2.$$

* * * (14) .

In the above equations, $\beta_m = \beta_m' + i\beta_m''$.

$$\beta_m'^2 = \frac{k_m^2 (1 + \sqrt{1 + \gamma_m^2})}{2},$$

$$\beta_m''^2 = \frac{k_m^2 (-1 + \sqrt{1 + \gamma_m^2})}{2}, \quad C_m = \sqrt{gH_m}.$$

Field Code Changed

Deleted: $\cos \beta_1 L_1 \cos \beta_2 L_2 = r \frac{p_1}{p_2} \sin \beta_1 L_1 \sin \beta_2 L_2$

Deleted: If $H_2 \ll H_1$ and $\cos \beta_1 L_1 \cos \beta_2 L_2 = 0$.

Deleted: .

Deleted: 1

Deleted: 2

Deleted: .

Deleted: 5

Deleted: .

Deleted: 5

Deleted: 2

Deleted: 5

Deleted: 1

Deleted: 2

Deleted: 2

Deleted: .

Deleted: 5

Deleted: 5

Deleted: 1

If we apply the quarter-wavelength resonance theory to channel 1, we can obtain resonant frequencies of 0.99 d^{-1} . If we apply the quarter-wavelength and three-quarter-wavelength resonance theories to channel 2 we can obtain resonant frequencies of 0.61 and 1.84 d^{-1} , respectively. Therefore, we can conclude that the major peaks around the frequency of 1.04 d^{-1} in Figure 6 are caused by resonance in channel 1. This indicates that channel 1 plays a determinative role in the two-channel system. Similarly, we can also conclude that the secondary and third peaks around the frequencies of 0.55 and 1.85 d^{-1} in Figure 6 are caused by resonances in channel 2, associated with the quarter-wavelength and three-quarter-wavelength resonances. Although the frequencies of the peaks shown in Figure 6 correspond well with those estimated based on the quarter-wavelength and three-quarter-wavelength theories, there are small discrepancies. This is due to the connection of the two channels. In fact, the resonant frequencies of the two-channel system also depend on the depth ratio of two channels, as shown in Eq. (14). In comparison to channel 2, the secondary, especially the third peak, in channel 1 is much more less significant. This can be explained as follows: The tidal incident wave from the channel 1 partially enters channel 2 across the steep topography at $x = 0$, and here, the rest of the wave is reflected. The reflected wave is superimposed with the incident wave, and tidal resonance occurs around the frequency of 1.04 d^{-1} . That is, the steep topography at $x = 0$ acts as a wall for channel 1, which causes the quarter-wavelength resonance to occur in the channel. Furthermore, the steep topography can also block most energy of the wave in channel 2 from entering channel 1. Therefore, the relatively large amplitudes in channel 2 at frequencies around 0.55 d^{-1} and 1.85 d^{-1} are not obvious in channel 1 under the action of friction.

Figure 7 displays the amplitude gains along the channels when channel 2 is in a resonant state. In this figure, the solution in presence/absence of friction is shown in panel a/b. The figure shows that when the forcing frequency is equal to 1.040 d^{-1} , which is the major resonant frequency, the amplitude gain gradually increases from the mouth towards the head in channel 1. In channel 2, the amplitude gain decreases first and reaches a trough before increasing again towards the head. The trough corresponds with the amphidromic zone of the diurnal tides in the GOT (see Figure 2a or the cotidal charts in Wu et al., 2015). For a frequency of 0.558 d^{-1} , the amplitude gain is nearly constant in channel 1 and increases with a relatively high rate towards the head in channel 2. For a frequency of 1.848 d^{-1} , the amplitude gain is also nearly constant in channel 1, and in channel 2, there are two antinodes and one node. This result is similar to the distribution of semi-diurnal tides in the GOT. When friction is neglected, the basic characteristics are the same, but the amplitude gain significantly increases.

6 Conclusions

The GOT is dominated by diurnal tides, indicating that the response near the diurnal tide frequency in the GOT is stronger than that at other frequencies. However, when applied to the GOT, the classical quarter-wavelength resonant theory fails to yield a diurnal resonant period. Changing the water depths in the SCSB in our numerical experiments further shows that the resonance of the SCSB has a critical impact on the resonance of the GOT. An idealised two-channel model that can reasonably explain the resonance in the GOT is established. Through the numerical experiments and two-channel model, we found that the resonant frequency around one cycle per day in the South China Sea main area can be explained with the

Deleted: 6

Deleted: .

Deleted: .

Deleted: 5

Deleted: Our study shows that this feature is mainly related to tidal resonance.

Deleted:

Deleted: in giving

Deleted: resonance

Deleted: in

Deleted: is closely related to the resonance in the SCSB

quarter-wavelength resonance theory, and the large-amplitude response at this frequency in the GOT is basically a passive response of the gulf to the increased amplitude of the wave in the southern portion of the main area of the South China Sea. However, there are still some problems that require further exploration, such as the effects of the length, width, depth, Coriolis force and friction of the SCSB on the GOT, which will be the focus of subsequent studies.

5 Code availability

In this paper, we use the Princeton Ocean Model (POM), which is available online at <http://www.ccpo.odu.edu/POMWEB/>.

Data availability

The ETOPO1 data (doi: 10.7289/V5C8276M) are available online at <https://www.ngdc.noaa.gov/mgg/global/>.

[The tidal data at the open boundaries are available online at ftp://ftp.oce.orst.edu/dist/tides.](ftp://ftp.oce.orst.edu/dist/tides)

10 Appendix: the analytical solution to the tidal wave equation for the two-channel model

In this appendix, we provide a detailed derivation process for the solution of the two-channel model presented in Section 5.

The following symbols are used in the derivation:

i : imaginary units

t : time

15 ω : angular velocity

g : gravitational acceleration

γ : frictional coefficient

$\tilde{\zeta}(x, t)$: water level

$\zeta(x)$: complex amplitude of the water level

20 $\tilde{u}(x, t)$: x -direction current velocity

$u(x)$: complex amplitude of the x -direction current velocity

k : wavenumber

H : water depth

L : length of the channel

25 $m = 1, 2$: different channel segments

The governing equation for tidal motion has the form (see Eq. (8) of the text):

Deleted: .

Deleted: shall give

Deleted: 4

Deleted: shall be

$$\begin{cases} -i\omega u_m = -g \frac{d\zeta_m}{dx} - \gamma_m u_m \\ -i\omega \zeta_m = -H_m \frac{du_m}{dx} \end{cases} \quad (A1)$$

Substituting the first equation into the second one, we obtain

$$\frac{d^2 \zeta_m}{dx^2} + \beta_m^2 \zeta_m = 0, \quad (A2)$$

where

$$\beta_m^2 = k_m^2 (1 + i\mu_m) \quad (A3)$$

In which $\mu_m = \frac{\gamma_m}{\omega}$ is a friction parameter and $k_m = \frac{\omega}{C_m}$ is the wavenumber with $C_m = \sqrt{gH_m}$ representing the wave velocity.

The solution to Eq. (A2) is

$$\zeta_m(x) = A_m e^{i\beta_m x} + B_m e^{-i\beta_m x}, \quad (A4)$$

10 where β_m can be expressed in the form

$$\beta_m = \beta_m' + i\beta_m'' \quad (\beta_m', \beta_m'' \text{ are real numbers}). \quad (A5)$$

$$\beta_m'^2 = \frac{k_m^2 (1 + \sqrt{1 + \mu_m^2})}{2}, \text{ and} \quad (A6)$$

$$\beta_m''^2 = \frac{k_m^2 (-1 + \sqrt{1 + \mu_m^2})}{2}. \quad (A7)$$

We can obtain the following solution of $u_m(x)$ from Eqs. (A1) and (A4):

$$15 \quad u_m(x) = \sqrt{\frac{g}{H_m}} (1 + i\mu_m)^{-\frac{1}{2}} (A_m e^{i\beta_m x} - B_m e^{-i\beta_m x}). \quad (A8)$$

Substituting the open boundary and matching conditions of the two channels (see Eqs. (9) to (11) in the text) into Eqs. (A4) and (A8), we obtain

Deleted:
$$\begin{cases} \frac{\partial \tilde{u}_m}{\partial t} = -g \frac{\partial \zeta_m}{\partial x} - \gamma_m \tilde{u}_m \\ \frac{\partial \zeta_m}{\partial t} = -H_m \frac{\partial \tilde{u}_m}{\partial x} \end{cases} \dots (A1)$$

where $\tilde{u}_m(x, t)$ and $\zeta_m(x, t)$ can be expressed in the following forms:

$$\tilde{u}_m(x, t) = Re(u_m(x) e^{-i\omega t}) \dots (A2)$$

$$\zeta_m(x, t) = Re(\zeta_m(x) e^{-i\omega t}) \dots (A3)$$

Eq. (A1) can be simplified as follows:

Deleted: 4

Deleted: From Eq. (A4)

Deleted: have

Deleted:
$$-i\omega \frac{du_m}{dx} = -g \frac{d^2 \zeta_m}{dx^2} - \gamma_m \frac{du_m}{dx} \dots (A)$$

5) Therefore, equivalently,

$$\frac{du_m}{dx} = g \frac{d^2 \zeta_m}{dx^2} (i\omega - \gamma_m)^{-1} \dots (A6)$$

The second equation in Eq. (4) yields:

$$\frac{du_m}{dx} = i\omega \zeta_m H_m^{-1} \dots (A7)$$

Deleted: 9

Deleted: 10

Deleted: ;

Deleted: 9

Deleted: ;

Deleted: 11

Deleted:

Deleted: 12

Deleted: ;

We can obtain the following equations from Eqs. (A10) and (A12) (...)

Deleted: 18

Deleted: 19

Deleted: Because Eq. (A11) includes either positive and negative (...)

Deleted: 4

Deleted: 11

Deleted: 22

Deleted: T

Deleted: are as follows:

$$B_2 = \frac{a_0}{2} R_0 e^{-i\beta_2 L_2},$$

where

$$R_0 = \frac{1}{\cos \beta_2 L_2 \cos \beta_1 L_1 - r \frac{P_1}{P_2} \sin \beta_1 L_1 \sin \beta_2 L_2}.$$

We can then obtain the value of A_2 :

$$A_2 = \frac{a_0}{2} e^{i\beta_2 L_2}.$$

Substituting Eqs. (A9) and (A11) into Eq. (A4) gives

$$\zeta_2(x) = a_0 R_0 \cos \beta_2 (x + L_2).$$

We can then obtain the expressions of the coefficients of $\zeta_1(x)$ as follows:

$$A_1 = \frac{1+r \frac{P_1}{P_2}}{2} \frac{a_0}{2} R_0 e^{i\beta_2 L_2} + \frac{1-r \frac{P_1}{P_2}}{2} \frac{a_0}{2} R_0 e^{-i\beta_2 L_2},$$

$$B_1 = \frac{1-r \frac{P_1}{P_2}}{2} \frac{a_0}{2} R_0 e^{i\beta_2 L_2} + \frac{1+r \frac{P_1}{P_2}}{2} \frac{a_0}{2} R_0 e^{-i\beta_2 L_2}.$$

Thus,

$$\zeta_1(x) = a_0 R_0 Q(x).$$

$$Q(x) = \cos(\beta_2 L) \cos(\beta_1 x) - r \frac{P_1}{P_2} \sin(\beta_2 L) \sin(\beta_1 x).$$

(A9)

Deleted: 39

(A10)

Deleted: 40

Deleted: through Eq. (A28):

(A11)

Deleted: 41

(A12)

Deleted: 39

Deleted: 40

Deleted: 11

Deleted: 42

Deleted:

Deleted: from Eqs. (A32), (A33), (A39) and (A40)

Deleted: 43

(A13)

Deleted: 44

(A14)

(A15)

Deleted: 45

(A16)

Field Code Changed

Competing interests

15 The authors declare that they have no conflicts of interest.

Acknowledgements

This study was supported by the National Key Research and Development Program of China (2017YFC1404200), the NSFC-Shandong Joint Fund for Marine Science Research Centers (Grant No. U1406404), and the Basic Scientific Fund for National Public Research Institutes of China (Grant No. 2015G02). [The authors sincerely thank the topic editor, Dr. Neil Wells for handling our manuscript. We also sincerely thank two referees for reviewing our manuscript. In particular, Dr. D. J. Webb thoroughly reviewed our manuscript and provided many useful comments and suggestions, which were of great help in improving our study.](#)

References

- Arbic, B. K., Karsten, R. H., and Garrett, C.: On tidal resonance in the global ocean and the back-effect of coastal tides upon open-ocean tides, *Atmos. Ocean.*, 47, 239–266, doi:10.3137/OC311.2009, 2009.
- Aungsakul, K., Jaroensutasinee, M., and Jaroensutasinee, K.: Numerical study of principal tidal constituents in the Gulf of Thailand and the Andaman Sea, *Walailak Journal of Science and Technology*, 4, 95–109, 2011.
- Cui, X., Fang, G., Teng, F., and Wu, D.: Estimating peak response frequencies in a tidal band in the seas adjacent to China with a numerical model, *Acta Oceanol. Sin.*, 34, 29–37, doi:10.1007/s13131-015-0593-z, 2015.
- 15 [Egbert G D, Erofeeva S Y.: Efficient inverse modeling of barotropic ocean tides, *Journal of Atmospheric and Oceanic Technology*, 19\(2\): 183-204, 2002.](#)
- Fang, G., Kwok, Y.-K., Yu, K., and Zhu, Y.: Numerical simulation of principal tidal constituents in the South China Sea, Gulf of Tonkin and Gulf of Thailand, *Cont. Shelf. Res.*, 19, 845–869, doi:10.1016/S0278-4343(99)00002-3, 1999.
- Garrett, C.: Tidal resonance in the Bay of Fundy and Gulf of Maine, *Nature*, 238, 441–443, doi:10.1038/238441a0, 1972.
- 20 Godin, G.: On tidal resonance, *Cont. Shelf. Res.*, 13, 89–107, doi:10.1016/0278-4343(93)90037-X, 1993.
- Miles, J., and Munk, W.: Harbor paradox, *Journal of the Waterways and Harbors Division*, 87, 111–130, 1961.
- Munk, W. H. and Cartwright, D. E.: Tidal spectroscopy and prediction, *Philos. T. R. Soc. S-A.*, 259, 533–581, 1966.
- Roos, P. C., Velema, J. J., Hulscher, S. J. M. H., and Stolk, A.: An idealised model of tidal dynamics in the North Sea: resonance properties and response to large-scale changes, *Ocean Dynam.*, 61, 2019–2035, doi:10.1007/s10236-011-0456-x, 2011.
- 25 Sirisup, S. and Kitamoto, A.: An unstructured normal mode decomposition solver on real ocean topography for the analysis of storm tide hazard, in: *Proceedings of the IEEE Oceans Conference*, Yeosu, South Korea, 21-24 May 2012, 1–7, 2012.
- Sutherland, G., Garrett, C., and Foreman, M.: Tidal resonance in Juan de Fuca Strait and the Strait of Georgia, *J. Phys. Oceanogr.*, 35, 1279–1286, doi:10.1175/JPO2738.1, 2005.
- 30 Teng, F., Fang, G. H., Wang, X. Y., Wei, Z. X., and Wang, Y. G.: Numerical simulation of principal tidal constituents in the Indonesian adjacent seas, *Advances in Marine Science*, 31, 166–179, 2013.

- Tomkratoke, S., Sirisup, S., Udomchoke, V., and Kanasut, J.: Influence of resonance on tide and storm surge in the Gulf of Thailand, *Cont. Shelf. Res.*, 109, 112–126, doi:10.1016/j.csr.2015.09.006, 2015.
- [Webb, D. J.: Notes on a 1-D model of continental shelf resonances, Research and Consultancy Report 85, National Oceanography Centre, Southampton, 2011.](#)
- 5 [Webb, D. J.: On the tides and resonances of Hudson Bay and Hudson Strait, Ocean Science, 10, 411-426, 2014.](#)
- Wei, Z., Fang, G., Susanto, R., Adi, T., Fan, B., Setiawan, A., Li, S., Wang, Y., and Gao, X.: Tidal elevation, current and energy flux in the area between the South China Sea and Java Sea, *Ocean Science*, 12, 517–531, doi:10.5194/os-12-517-2016, 2016
- 10 Wu, D., Fang, G., and Cui, X.: Tides and tidal currents in the Gulf of Thailand in a two-rectangular-Gulf model, *Advances in Marine Science*, 31, 465–477, 2013.
- Wu, D., Fang, G., Cui, X., and Teng, F.: Numerical simulation of tides and tidal currents in the Gulf of Thailand and its adjacent area, *Acta. Oceanol. Sin.*, 37, 11–20, 2015.
- Yanagi, T. and Takao, T.: Clockwise phase propagation of semi-diurnal tides in the Gulf of Thailand, *J. Oceanogr.*, 54, 143–150, doi:10.1007/bf02751690, 1998.
- 15 Zu, T., Gan, J., and Erofeeva, S. Y.: Numerical study of the tide and tidal dynamics in the South China Sea, *Deep Sea Research Part I: Oceanographic Research Papers*, 55, 137–154, doi:10.1016/j.dsr.2007.10.007, 2008.

Figure captions

Figure 1: The South China Sea and its neighbouring area. The contours show the water depth distribution in metres. The blue line B is the mouth cross section of the Gulf of Thailand (GOT). The triangles represent the tidal gauge stations (the full names of these stations are given in Table 1). The inset in the upper-left corner shows the entire model domains (99-131 E, 1.5-42 N).

5 **Figure 2:** Model-produced K_1 tidal system. (a) The distribution of Greenwich phase-lags (in degrees) and amplitudes (colour, in metres). (b) Tidal energy flux density vectors (in kW m^{-2}).

Figure 3: Response functions (amplitude gains as a function of frequency) of the South China Sea body (SCSB) (a) and the Gulf of Thailand (GOT) (b) for different bottom topographies. Here, the amplitude gains refer to the area-means of the top 20% values. The definition of the experiments is given in Table 2.

10 **Figure 4:** (a) Distribution of amplitude gain (colour) and phase change (lines in degrees) for the frequency of 0.99 cycle per day; (b) corresponding energy flux density vectors.

Figure 5: The two-channel model configuration representing the SCSB-GOT system.

Figure 6: Response function at the locations $x = -L_2$ (a) and $x = 0$ (b) with and without friction.

Figure 7: The amplitude gain as a function of x for different peak frequencies with friction (a) and without friction (b).

15

Deleted: :

Deleted: Study area. The contours show the water depth distribution in meters. The red line B is the mouth cross section of the Gulf of Thailand (GOT).

Deleted: :

Deleted: : .

Deleted: 2

Deleted: :

Deleted: of the SCSB

Deleted: Figure 3: Comparison of the response functions of the SCSB with and without the GOT. .

Deleted: 4

Deleted: :

Deleted: 5

Deleted: :

Deleted: 6

Deleted: :

Tables

Table 1. Comparison between model-produced and observed K₁ tidal amplitudes (m) and phase-lags (degrees refer to Greenwich time).

No.	Place	E	N	Model		Tidal gauge observation	
				Amp. (m)	Phase-lag °	Amp. (m)	Phase-lag °
<u>1</u>	<u>Makung</u>	<u>119.57 E</u>	<u>23.59 N</u>	<u>0.25</u>	<u>138</u>	<u>0.25</u>	<u>158</u>
<u>2</u>	<u>Hong Kong</u>	<u>114.17 E</u>	<u>22.30 N</u>	<u>0.36</u>	<u>157</u>	<u>0.36</u>	<u>177</u>
<u>3</u>	<u>Hailingshan</u>	<u>111.82 E</u>	<u>21.58 N</u>	<u>0.40</u>	<u>175</u>	<u>0.42</u>	<u>194</u>
<u>4</u>	<u>Naozhou I</u>	<u>110.58 E</u>	<u>20.95 N</u>	<u>0.41</u>	<u>199</u>	<u>0.44</u>	<u>205</u>
<u>5</u>	<u>Basuo</u>	<u>108.62 E</u>	<u>19.10 N</u>	<u>0.60</u>	<u>299</u>	<u>0.54</u>	<u>311</u>
<u>6</u>	<u>Lingshuijiao</u>	<u>110.07 E</u>	<u>18.38 N</u>	<u>0.32</u>	<u>176</u>	<u>0.30</u>	<u>197</u>
<u>7</u>	<u>Quang Khe</u>	<u>106.47 E</u>	<u>17.70 N</u>	<u>0.36</u>	<u>351</u>	<u>0.21</u>	<u>350</u>
<u>8</u>	<u>Qui Nhon</u>	<u>109.22 E</u>	<u>13.75 N</u>	<u>0.34</u>	<u>169</u>	<u>0.34</u>	<u>195</u>
<u>9</u>	<u>Vung Tau</u>	<u>107.07 E</u>	<u>10.33 N</u>	<u>0.58</u>	<u>187</u>	<u>0.61</u>	<u>207</u>
<u>10</u>	<u>Con Dao</u>	<u>106.63 E</u>	<u>8.67 N</u>	<u>0.55</u>	<u>208</u>	<u>0.64</u>	<u>213</u>
<u>11</u>	<u>Kamau River</u>	<u>104.75 E</u>	<u>8.65 N</u>	<u>0.34</u>	<u>257</u>	<u>0.37</u>	<u>245</u>
<u>12</u>	<u>Hatien</u>	<u>104.47 E</u>	<u>10.37 N</u>	<u>0.26</u>	<u>312</u>	<u>0.26</u>	<u>321</u>
<u>13</u>	<u>Kaoh Kong I</u>	<u>103.00 E</u>	<u>11.42 N</u>	<u>0.33</u>	<u>30</u>	<u>0.37</u>	<u>41</u>
<u>14</u>	<u>Chandaburi</u>	<u>102.07 E</u>	<u>12.47 N</u>	<u>0.47</u>	<u>44</u>	<u>0.58</u>	<u>54</u>
<u>15</u>	<u>Satahib bay</u>	<u>100.92 E</u>	<u>12.65 N</u>	<u>0.55</u>	<u>60</u>	<u>0.64</u>	<u>56</u>
<u>16</u>	<u>Ko Raet</u>	<u>99.82 E</u>	<u>11.80 N</u>	<u>0.46</u>	<u>60</u>	<u>0.52</u>	<u>64</u>
<u>17</u>	<u>Tumpat</u>	<u>102.17 E</u>	<u>6.20 N</u>	<u>0.29</u>	<u>236</u>	<u>0.28</u>	<u>231</u>
<u>18</u>	<u>Trengganu</u>	<u>103.13 E</u>	<u>5.35 N</u>	<u>0.47</u>	<u>242</u>	<u>0.52</u>	<u>243</u>
<u>19</u>	<u>Kuantan</u>	<u>103.33 E</u>	<u>3.83 N</u>	<u>0.52</u>	<u>257</u>	<u>0.52</u>	<u>258</u>
<u>20</u>	<u>Pulau Tioman</u>	<u>104.13 E</u>	<u>2.80 N</u>	<u>0.47</u>	<u>272</u>	<u>0.49</u>	<u>265</u>
<u>21</u>	<u>Anamba Is.</u>	<u>106.25 E</u>	<u>3.23 N</u>	<u>0.37</u>	<u>257</u>	<u>0.40</u>	<u>253</u>
<u>22</u>	<u>Pulau Laut</u>	<u>108.00 E</u>	<u>4.75 N</u>	<u>0.37</u>	<u>221</u>	<u>0.36</u>	<u>228</u>
<u>23</u>	<u>Natuna</u>	<u>108.03 E</u>	<u>3.80 N</u>	<u>0.31</u>	<u>235</u>	<u>0.40</u>	<u>235</u>
<u>24</u>	<u>Subi Kechil</u>	<u>108.85 E</u>	<u>3.05 N</u>	<u>0.28</u>	<u>234</u>	<u>0.37</u>	<u>230</u>
<u>25</u>	<u>Tanjong Datu</u>	<u>109.65 E</u>	<u>2.08 N</u>	<u>0.29</u>	<u>207</u>	<u>0.37</u>	<u>215</u>
<u>26</u>	<u>Kota Kinabalu</u>	<u>115.98 E</u>	<u>5.87 N</u>	<u>0.39</u>	<u>175</u>	<u>0.35</u>	<u>194</u>
<u>27</u>	<u>Ulugan bay</u>	<u>118.77 E</u>	<u>10.07 N</u>	<u>0.34</u>	<u>174</u>	<u>0.34</u>	<u>197</u>

<u>28</u>	<u>Lubang I.</u>	<u>120.20 ₱</u>	<u>13.82 ₱</u>	<u>0.30</u>	<u>173</u>	<u>0.29</u>	<u>190</u>
<u>29</u>	<u>Santa Cruz</u>	<u>119.90 ₱</u>	<u>15.77 ₱</u>	<u>0.28</u>	<u>173</u>	<u>0.26</u>	<u>193</u>
<u>30</u>	<u>San Fernando</u>	<u>120.30 ₱</u>	<u>16.62 ₱</u>	<u>0.25</u>	<u>173</u>	<u>0.24</u>	<u>192</u>
<u>31</u>	<u>Yongshujiao</u>	<u>112.88 ₱</u>	<u>9.55 ₱</u>	<u>0.35</u>	<u>173</u>	<u>0.35</u>	<u>191</u>

Table 2 Resonant frequencies and periods obtained from the six experiments.

Exp	Topography		Resonant frequency /d ⁻¹		Resonant period /h	
	SCSB	GOT	SCSB	GOT	SCSB	GOT
1	Real depth	Real depth	0.99	1.01	24.36	23.79
2	Halved depth	Real depth	0.75	0.75	32.00	32.00
3	Doubled depth	Real depth	1.49	1.50	16.10	16.00
4	Real depth	Halved depth	0.99	1.01	24.36	23.79
5	Real depth	Doubled depth	0.99	1.01	24.36	23.79
6	Real depth	Section-B closed	1.01	-	23.79	-

Deleted: 1

Deleted: four

Deleted: f

Deleted: Twice

Table 3. The resonant frequencies and corresponding periods at $x = -L_2$ and $x = 0$.

Solution	$x = -L_2$						$x = 0$					
	Peak frequency /d ⁻¹			Peak period /h			Peak frequency /d ⁻¹			Peak period /h		
1	0.558	1.040	1.848	43.01	23.08	12.99	-	1.040	-	-	23.08	-
2	0.545	1.044	1.856	44.04	22.99	12.93	0.545	1.044	1.856	44.04	22.99	12.93

Notes: Solution 1 and 2 are respectively for the cases in the presence and in the absence of friction

Deleted: 2

Figures

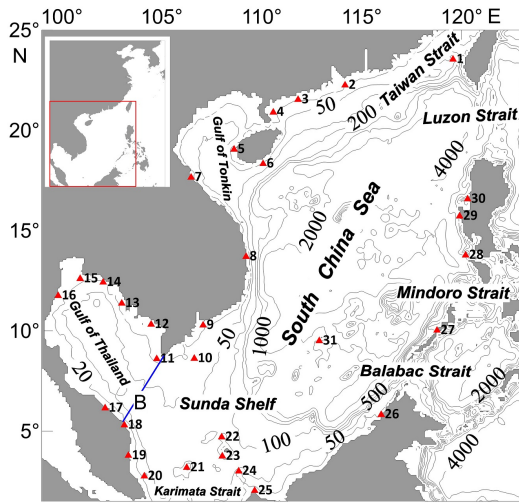
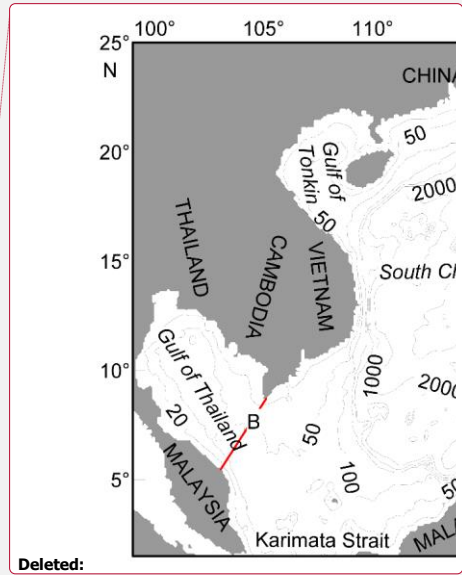


Figure 1. The South China Sea and its neighbouring area. The contours show the water depth distribution in metres. The blue line B is the mouth cross section of the Gulf of Thailand (GOT). The triangles represent the tidal gauge stations (the full names of these stations are given in Table 1). The inset in the upper-left corner shows the entire model domains (99-131 E, 1.5-42 N).

5



Deleted:

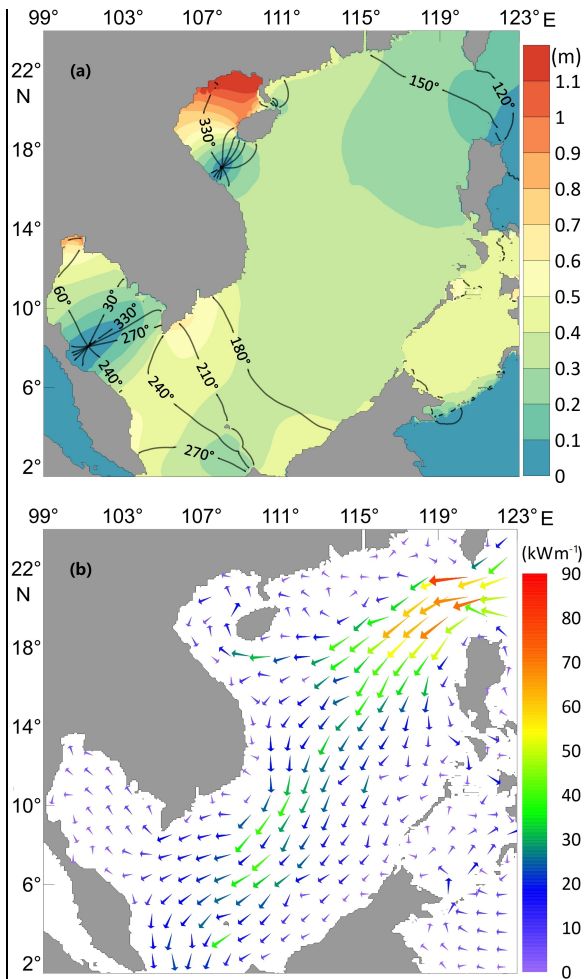
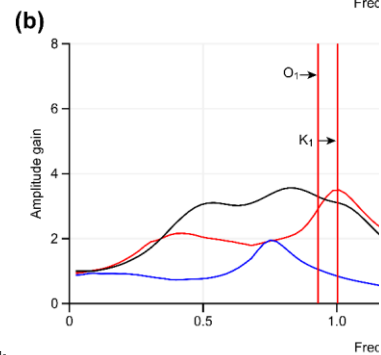
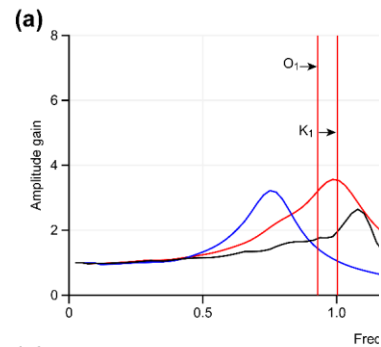


Figure 2. Model-produced K₁ tidal system. (a) The distribution of Greenwich phase-lags (in degrees) and amplitudes (colour, in metres). (b) Tidal energy flux density vectors (in kW/m²).



Deleted:

Formatted: Font: (Default) Times New Roman

Deleted:

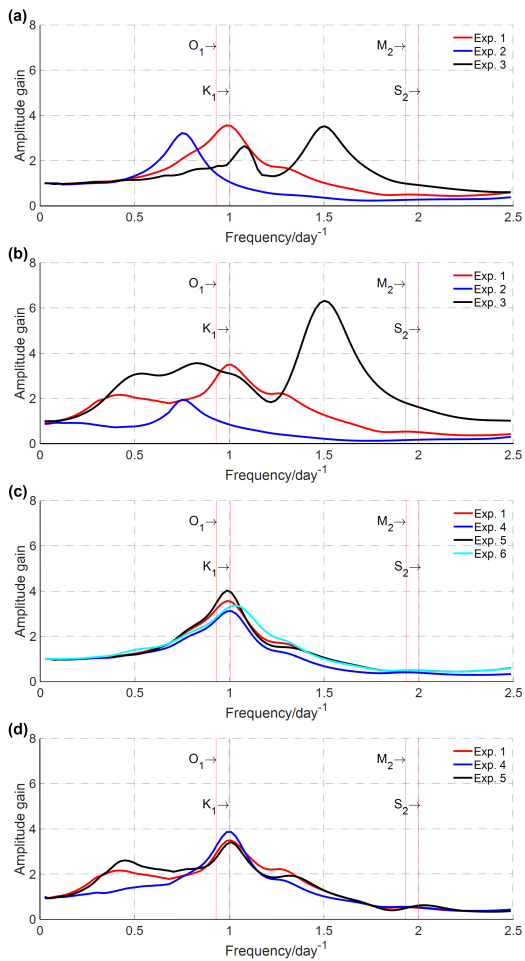
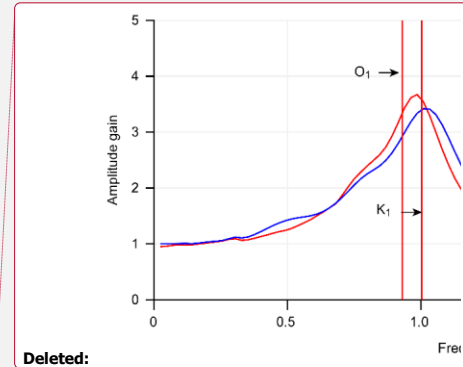


Figure 3. Response functions (amplitude gains as a function of frequency) of the South China Sea body (SCSB) (a) and the Gulf of Thailand (GOT) (b) for different bottom topographies. Here, the amplitude gains refer to the area-means of the top 20% values. The definition of the experiments is given in Table 2.



Deleted:

Deleted: Figure 3 .

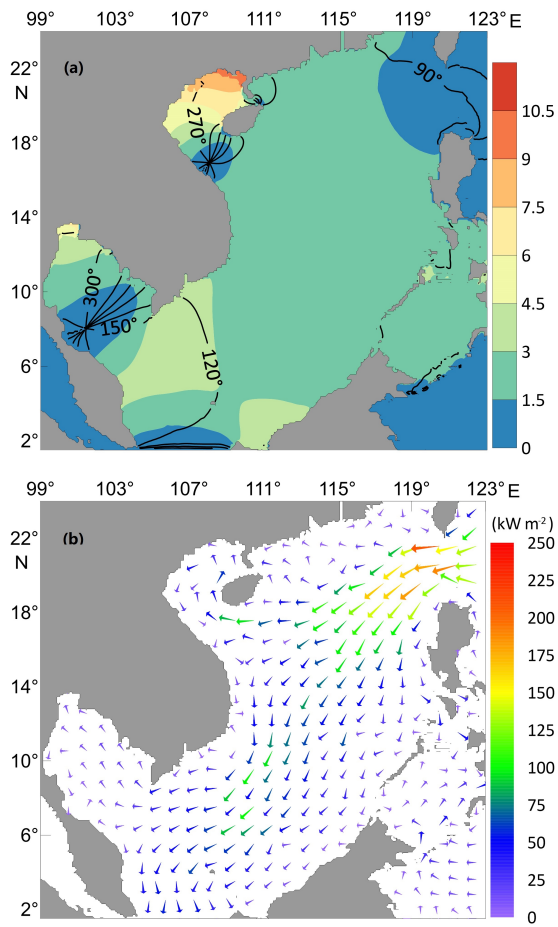


Figure 4. (a) Distribution of amplitude gain (colour) and phase change (lines in degrees) for the frequency of 0.99 cycle per day; (b) corresponding energy flux density vectors.

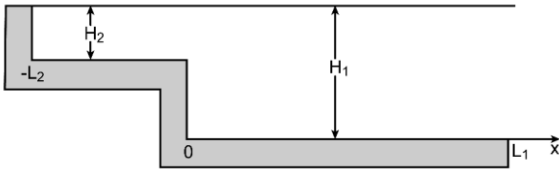


Figure 5. The two-channel model configuration representing the SCSB-GOT system.

Deleted: 4

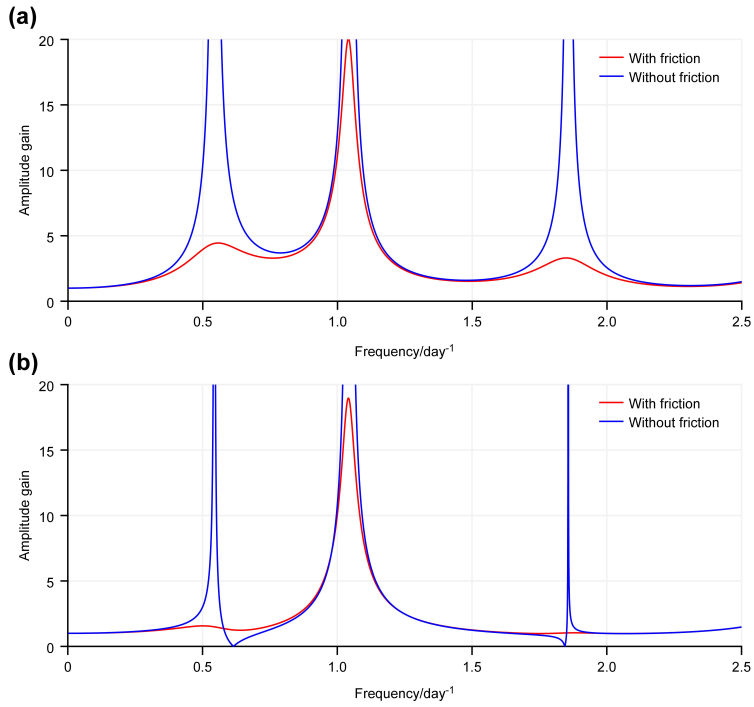


Figure 6. Response function at the locations $x = -L_2$ (a) and $x = 0$ (b) with and without friction.

Deleted: 5

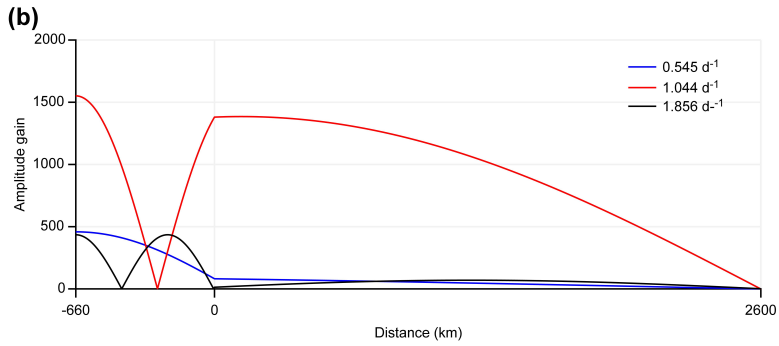
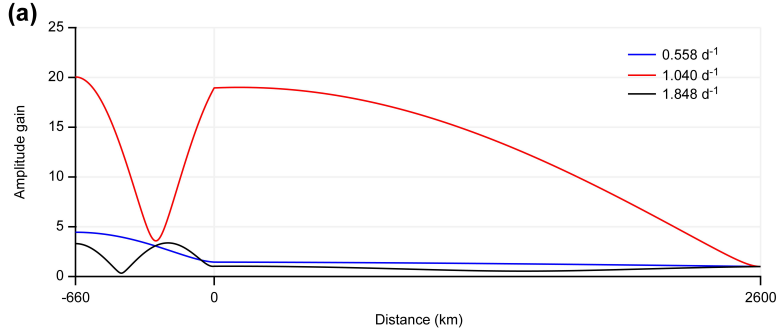


Figure 7. The amplitude gain as a function of x for different peak frequencies with friction (a) and without friction (b).

Deleted: 6